

# One- and Two-Sided Burning of Thermally Thin Materials

T. Ohlemiller and J. Shields

Building and Fire Research Laboratory, National Institute of Standards and Technology, Gaithersburg, MD 20899, USA

The rate of heat release from a thermally thin material burning on both sides will be more than twice the value seen when only one side is burning. Two simplified models demonstrate that this is a consequence of the Arrhenius temperature dependence of the gasification rate of the solid. Experiments carried out on three composite materials over a range of incident heat fluxes confirm this effect. It is inferred that a further consequence of this heat release enhancement is an increased tendency for concurrent flame spread in the two-sided burning case. Materials whose application could lead to two-sided burning should thus be assessed in this mode to obtain a true picture of their flammability potential.

## INTRODUCTION

In spacecraft applications, many slab-like materials are dimensionally thin as a result of weight considerations. In terrestrial applications, thin materials are encountered in clothing, draperies, paper, electronic circuit boards, etc. These materials may be expected to approach thermally thin behavior during combustion. By thermally thin is meant that heat absorbed on one surface of the material will penetrate its thickness sufficiently rapidly so that there will be no significant temperature gradient through the material depth. The specific criteria for such behavior are addressed below.

In testing the flammability of a material it is important to measure the worst behavior it is likely to exhibit in the application of interest. For any application of a slab-like material it is pertinent to ask whether simultaneous burning on both surfaces is possible; this is clearly worse than the burning of one surface only. When this occurs with a dimensionally thick material the result is a doubling of the burning rate or overall rate of heat release because twice as much surface area is involved. This simple factor of two relationship pertains because such dimensionally thick materials typically are also thermally thick. The heat wave in the material from the burning of each surface does not extend past the center plane through the material. As a result, the two burning surfaces are thermophysically isolated and do not interact. (There could be other interactions in a real application, such as competition of the two burning surfaces for the same oxygen supply.) For dimensionally thin materials, the approach to thermally thin behavior implies just the opposite: the thermal waves from the two burning surfaces merge to the point of producing a uniform temperature through the depth of the material. In this case the thermophysical interaction between the burning zones is a maximum. The heat feedback from the flame on one surface is felt by both burning surfaces and there is an enhancement of the burning rate that is greater than a factor of two. The details behind this are encompassed in the models discussed below. From a fire safety point of view, this means that two-sided burning on thin materials is more hazardous than one might initially expect. Thus

any thin material which conceivably could burn on both surfaces in a spacecraft or terrestrial application should be tested in this way (even if such burning would require the failure of some initial bonding to a nominally protective second surface).

The specific application of these ideas in this work has been in the measurement of the rate of heat release from thin materials burning on one or two sides while irradiated in the NIST Cone Calorimeter apparatus. Specific details of that apparatus add certain complications to the measurements, as will be seen. First, however, the basis for the thermally thin enhancement of burning rate (or heat release rate) will be examined in the context of two models.

## SIMPLIFIED MODELS FOR BURNING OF THERMALLY THIN MATERIALS

### Steady-state model

The qualitative essence of the problem can be seen in a simple steady-state energy balance. Consider two different burning conditions for a thermally thin material: (1) the material is irradiated with a constant flux on one surface and is burning on that surface only; (2) the material is irradiated on both surfaces and is burning on both surfaces also. The external radiation is included for the usual reason in flammability assessment, i.e. it simulates a nearby burning object, self-feedback of radiation from a burning surface with a concave geometry or, less quantifiably, the increased flame feedback attendant to larger-scale fires. In case (1) the material is gasifying from both sides at an equal rate but only half of those gasification products are burning. This is so because the degradation and gasification of the solid fuel is a volumetric process, not a surface process. Since, in a thermally thin material, the temperature is constant throughout the depth, the gasification rate is also and the products tend to depart equally from both surfaces.

The use of a steady-state argument for a thermally thin material is an artifice. Fuel depletion is inherently import-

ant in such a thin fuel and so the process is necessarily transient. Depletion is included in the second model below. Here the steady-state result can be thought of as an approximation to the peak value (of burning rate or rate of heat release) seen experimentally. The approximation is rough but the simple model is instructive nonetheless.

For case (1), burning on one side only, the steady-state heat balance becomes:

$$q_{\text{ext}} + \zeta h (T_f - T_s) = Q_s l_s Z_s \exp(-E/RT_s) + \sigma(T_s^4 - T_o^4) \quad (1)$$

Here  $q_{\text{ext}}$  is the external radiant flux; the material is assumed to have a negligible reflectivity for this flux. The second term in Eqn (1) is the convective heat feedback from the flame whose temperature is  $T_f$  (taken to be independent of incident heat flux);  $h$  is the convective heat transfer coefficient between flame and sample surface and the quantity  $\zeta$  is a correction to this for blowing of the flame in the buoyant boundary layer. This is dependent on the mass flux from the surface and is computed from an expression derived by Spalding:<sup>1</sup>

$$\zeta = (\dot{m} C_g / h) / [\exp(\dot{m} C_g / h) - 1] \quad (2)$$

Here  $\dot{m}$  is the mass flux from the surface (one half of the total gasification rate throughout the sample depth) and  $C_g$  is the heat capacity of the gas. The value of  $\zeta$  varies from zero for an infinite gasification rate to one for no gasification. The two heat sources on the left in Eqn (1) are balanced by the two heat sinks on the right. The first term on the right is the heat required to gasify the solid fuel:  $Q_s$  is the heat of gasification (endothermic),  $l_s$  is the sample thickness,  $Z_s$  and  $E$  are kinetic parameters of the gasification process,  $R$  is the gas constant,  $T_s$  is the sample temperature. This first term on the right, with the reaction heat  $Q_s$  omitted, is the total volumetric gasification rate (twice the value of  $\dot{m}$  in Eqn (2)). The last term in Eqn (1) is the net radiative loss from the front surface of the sample;  $\sigma$  is the Stefan-Boltzmann constant and  $T_o$  is the ambient temperature. The rear surface of the sample is assumed to be adiabatic.

For case (2), both surfaces irradiated and burning, the steady-state heat balance is very similar.

$$2q_{\text{ext}} + 2\zeta h (T_f - T_s) = Q_s l_s Z_s \exp(-E/RT_s) + 2\sigma(T_s^4 - T_o^4) \quad (3)$$

Here all of the symbols have the same meaning as in the previous case.

Equations (1) and (3) are transcendental algebraic equations which define the steady-state value of  $T_s$ , the sample temperature; this in turn defines the rate of gasification of the sample and its heat release rate (gasification rate times heat of combustion of the gases). Clearly, the two physical situations will not lead to the same value for  $T_s$ ; this temperature will be higher for case (2) above because of the doubling of the heat source terms. The tendency for  $T_s$  to increase as a result of this heat source doubling is damped by the increased radiative loss (also doubled) and the tendency for the parameter  $\zeta$  to decrease when the mass flux from the surface tries to increase (the

flame is blown further out from the surface and thus heats it less effectively).

The equations for these two cases have been solved by a Newton-Raphson iteration technique to find  $T_s$ . The parameters have been chosen to be similar to those in the experiments described below, but are not identical, particularly since the gasification kinetics of the materials used there have not been determined. The values of the convective heat transfer coefficient (approximately  $50 \text{ kW m}^{-2} \text{ K}$ ) and the flame temperature ( $1500 \text{ K}$ ) were chosen so as to put the flame heat feedback flux in the right neighborhood (approximately  $30 \text{ kW m}^{-2}$ ). The kinetic parameters were chosen so that the overall gasification rate is comparable to that measured experimentally. The gasification heat used was a rather generic value ( $200 \text{ cal g}^{-1}$  or  $840 \text{ J g}^{-1}$ ). To compute a rate of heat release from the gasification rate, a heat of combustion comparable to that seen experimentally was used ( $20 \text{ kJ g}^{-1}$ ).

Since this tendency for the sample temperature to vary with heat input rate is a consequence of the Arrhenius temperature dependence of the gasification rate, the activation energy,  $E$ , was varied to assess its impact. When this was done, the value of  $Z_s$  was adjusted so as to keep the gasification rate at  $400 \text{ C}$  a constant value; otherwise a very artificial sensitivity would have been seen. This temperature, though somewhat arbitrary, is close to what one expects for the materials studied here.

At this point it is necessary to point out one of the complications that the experimental apparatus introduces. The apparatus (described in detail below) cannot separate gases evolved from the front or from the back of the sample and gases can freely evolve from both sides (in spite of an insulated rear surface—see below). The vertically oriented sample sits on a weight cell so that the total weight loss rate is seen. Furthermore, the gases which come from the back of the sample during one-sided heating inevitably burn when they meet the front face flame at the top of the sample (this top flame does not feed heat back to the rear surface of the sample). Thus the heat release seen in the one-sided case is double the value that the model above (Eqn (1)) implies. Because the model results are later to be compared with experimental results,

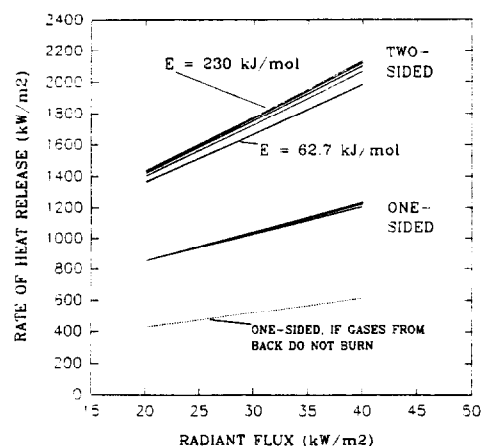


Figure 1. Steady-state model result: one- and two-sided heating/burning.

the former were expressed on the same basis, i.e. the rate of heat release reported here for case (1) is twice the value one would get if the premises of the model were strictly adhered to.

Figure 1 shows the result of solving the two cases and calculating the rate of heat release in the manner just indicated. The incident radiant flux has been varied over a range comparable to that used experimentally. One sees that the behavior is not greatly sensitive to the value of the activation energy,  $E$ . The two-sided heating/burning case is predicted by this steady-state model to yield somewhat less than a factor of two increase in rate of heat release for the conditions of the experiments described below. If the gases from the rear of the sample did not burn, the one-sided rates of heat release would be half the values shown by the solid lines; the dashed line shows where they would fall. The predicted ratio of heat release rate between the two cases would then be greater than three. Recall that the thermally thick case would yield only a factor of two.

### Transient model

The most unrealistic physical element of the preceding model is the neglect of solid fuel consumption. It does contain those essential features of the real problem necessary to demonstrate the origin of the burning rate enhancement when a thermally thin material is burning on both sides. However, the real problem is inherently transient because fuel is being consumed even as the sample proceeds from ignition toward a peak burning rate condition; this affects the value of that peak. Thus the preceding model is missing features which could affect the quantitative prediction of the ratio between one- and two-sided burning rates.

The only new elements in the transient model are the changing heat content of the solid fuel and its changing mass. To deal with these requires the simultaneous solution of two, coupled ordinary differential equations which express the conservation of energy and solid fuel mass. Most of the terms in the energy balance are again the same. Both the one- and two-sided heating/burning cases can be expressed by the single set of the following equations:

$$(\rho_s C_s l_s) dT_s/dt = f[q_{ext} + \zeta h(T_f - T_s) - \sigma(T_s^4 - T_\infty^4)] - Q_s l_s Z_s (\rho_s - \rho_{res}) \exp(-E/RT_s) \quad (4)$$

$$d\rho_s/dt = -Z_s (\rho_s - \rho_{res}) \exp(-E/RT_s) \quad (5)$$

The first term in Eqn (4) is the transient heat content of the solid fuel. The terms on the right-hand side of this equation are essentially the same as in the steady-state models. The quantity  $\zeta$  is given by Eqn (2) as before. The factor  $f$  is one for the one-sided heating/burning case and two for the two-sided case. The fuel concentration in the solid is now expressed explicitly in the fuel gasification rate term; it was implicit in  $Z_s$  in the steady-state models since it was not a variable as it is here. The quantity  $\rho_{res}$  is the residual mass of the sample after all the fuel is consumed. This has been introduced because all of the experimental samples are composite materials with a substantial glass-fiber content. Equation (5) expresses the conservation of solid fuel mass.

In order to implement this model a statement has to be made about when the flame appears (flaming ignition). A complete description of the runaway to flaming in the gas phase would require a much more complex model. Instead, use is made of the idea that there is a critical fuel mass flux level at which the flame appears;<sup>2</sup> in the experiments there is a spark igniter which ignites the gases as soon as they reach a flammable concentration. This simplification should be quite adequate for this model.

The equations are solved by an explicit time-marching method (fourth-order Runge-Kutta) starting from the first appearance of the flame. Since the mass flux at this point is prescribed ( $2.5 \text{ gm}^{-1} \text{ s}$ , from reference 2), the temperature and initial density can also be determined, assuming negligible reactant consumption prior to ignition. The model could be used to predict the time it takes the external radiant flux to raise the sample to this 'ignition temperature' but that is tangential to the main objective here.

Time steps of 1/16 second give energy and mass balance errors no greater than a few tenths of a per-cent. When fuel consumption is artificially suppressed this program converges to the same steady-state solutions as does the steady-state model above.

Figures 2-4 show the output of a typical case predicted by the transient model. The parameters not shown explicitly have the same values as those used in the steady-state model predictions. Figure 2 shows that the temperature of the sample climbs continually from the moment of ignition while Fig. 3 indicates that the fuel mass decays monotonically. The result, in Fig. 4, is a rate of heat release that goes through a peak about midway through the burning process. Burning is terminated in the model when the mass flux from the surface again drops to the critical level for flaming. Figure 5 shows that the time that the heat release rate peak is reached is sensitive to the activation energy of the gasification process; the height of the peak is weakly sensitive to this parameter.

Figure 6 shows a set of results from the transient model that is comparable to the steady-state set in Fig. 1. The more realistic transient model predicts lower peak rates of heat release. It also indicates a factor somewhat less than two between the rates of heat release from the one- and

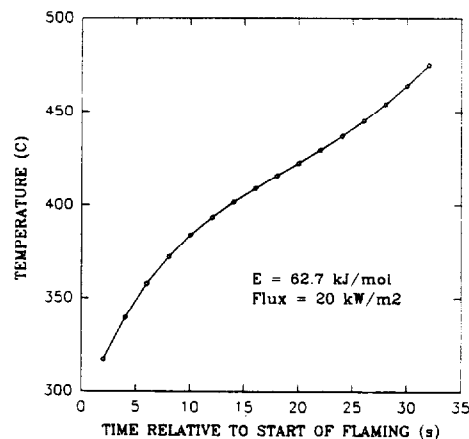


Figure 2. Transient model result: one-sided heating/burning.

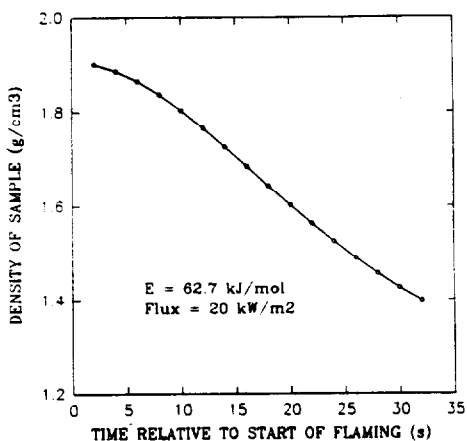


Figure 3. Transient model result: one-sided heating/burning.

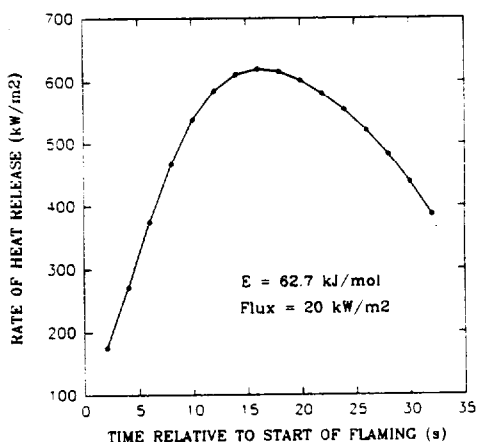


Figure 4. Transient model result: one-sided heating/burning.

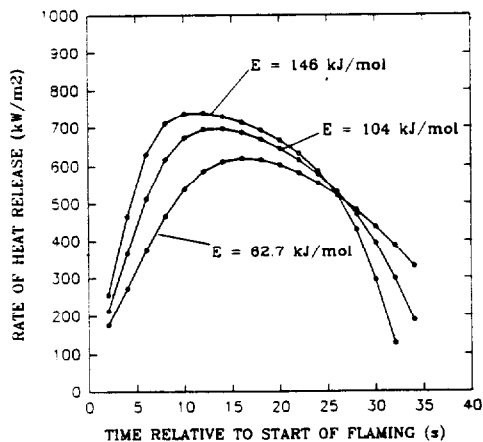


Figure 5. Transient model result: effect of activation energy on rate of heat release.

two-sided cases. Recall that the one-sided results as shown here assume the gases from both sides contribute to the reported rate of heat release. The dashed line shows where the one-sided results would fall if the gases from the back of the sample did not contribute to the rate of heat

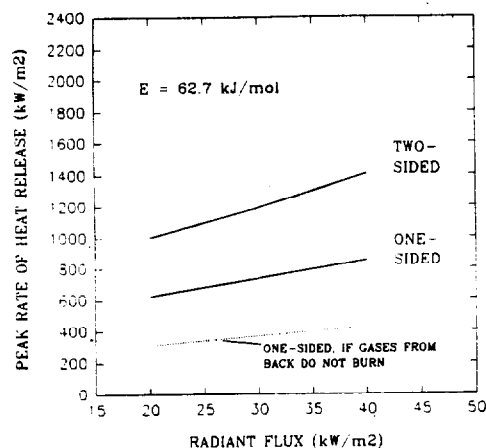


Figure 6. Transient model result: one- and two-sided heating/burning.

release. Comparison of the position of the dashed line with the two-sided results shows that there is still a factor greater than three between the one- and two-sided heating/burning cases. A comparison of these predictions with experimental measurements is made below.

## EXPERIMENTAL DETAILS

The NIST Cone Calorimeter is a device which measures rate of heat release from a burning object using oxygen-consumption calorimetry. The plume of products from the burning object is captured completely. Its flow rate and oxygen content are monitored continuously (5-second intervals). From these data and the fact that nearly all organic compounds evolve essentially the same amount of heat per gram of oxygen consumed, one can infer the rate of heat release to an accuracy of about  $\pm 5\%$ .

This device was designed to irradiate and measure samples burning on one side only. To use it for the present work it was necessary to remove the cone-shaped heating element and design a new device that could irradiate both sides of a thin, vertically oriented sample simultaneously (and equally). The device that was built for this purpose is shown schematically in Fig. 7: It consists of a matched pair of planar radiative heater assemblies, each 178 mm square, oriented vertically in a suitable holder with a gap of 32 mm. The heat source within each heater assembly is a 2500-W heater cable shaped into a zig zag pattern. Nickel elements placed between each rung of this pattern serve to spread the heat by conduction and pass it to nickel sheets (178 mm square) which form the face of each heater assembly. Each heater assembly is run by a constant temperature controller. The heat flux from each face can be measured by a Schmidt-Boelter gage placed at the same position as the center of the sample face. The system was designed to impose a uniform heat flux on a sample whose exposed face is 76 mm square. Actual measurements show the deviations above the horizontal centerline of the sample were about 3%; below the centerline they were 5%. The dynamics of the heater control were such that some upward drift in heater

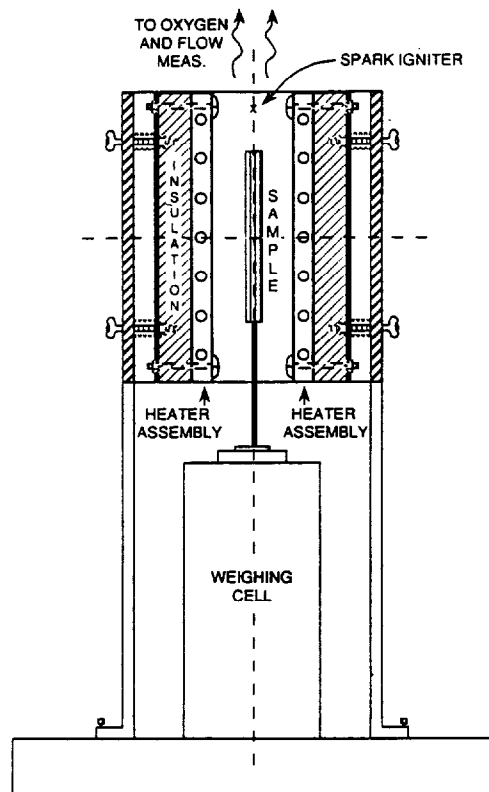


Figure 7. Apparatus for one- and two-sided burning of samples in the Cone Calorimeter.

temperature (5–10°C) occurred during sample exposure; this yields a change in the incident heat flux of less than 5%.

The samples, all 1.6 mm thick, were 82.5 mm square. The 1.25 mm peripheral edge surrounding the exposed face was loosely held between a minimal framework cut from 0.51 mm thick stainless steel sheet to reduce heat sinking on the sample edges.

All three of the samples tested were composite materials (see Table 1). Previous experience with composites has shown that they have a distinct tendency to develop internal bubbles during intense thermal degradation which then can lead to erratic jets of gases emerging at unpredictable times and locations. To eliminate this tendency, all samples had a pattern of very small holes drilled through them (1.3 mm dia.). Preliminary experiments established that a hole spacing of 6 mm yielded only weak gas jets which tended to merge into an essentially continuous flame sheet on the face(s) of the sample. This precluded practically all contact of the sample flames with the radiant heaters.

The vertical orientation of the samples (necessary to yield equal flames on the two faces) yielded a buoyant boundary layer which preferentially cooled the lowest portion of the sample face, countering the radiant heating somewhat, prior to ignition. This is a two-dimensional effect not included in the models above. As a consequence of this slightly lesser net heating rate for the lower portion of the sample, ignition tended to occur first on the upper half to two thirds of the irradiated face(s). The flame then spread down to envelop the entire face. When the rate of

Table 1. Description of test materials in one- versus two-sided burning study

Material	Thickness (mm)	Description
Haysite ETS <sup>a</sup>	1.6	A thermoset polyester reinforced with swirl mat glass fiber; organic resin content 37% by weight; 160 C mechanical rating.
Haysite H755	1.6	Polyester resin reinforced with swirl mat glass fiber; organic resin content 38% by weight; 165 C mechanical rating.
Epoxy/glass circuit board	1.6	G-11 NEMA rating (unretarded); woven roving glass; organic resin content 32% by weight; 177°C operating temperature rating.

<sup>a</sup> Haysite Reinforced Plastics, Inc., Erie, Pennsylvania 16509, USA.

heat release per unit area is computed from the raw experimental data it is normally assumed that the full face is burning from ignition onward. The focus here is primarily on the peak burning condition (peak rate of heat release). Most of the tests were video-taped so that the extent of sample face burning could be determined as a function of time. In some cases, the full face was not burning when the peak heat release rate was reached. The worst case was about 90% area involvement at the time the peak occurred; the peak values reported here have been corrected for this effect when the tapes showed it was present. This correction, which is for the actual burning area only, cannot fully eliminate the effects of non-simultaneous ignition of the full sample face. The peak is also lowered somewhat by the fact that the area which first ignited has undergone some fuel depletion by the time the lower portion of the sample face is fully ignited.

Recall that the model assumes that the one-sided burning case is adiabatic on the non-irradiated face. Also, half of the gases generated within the sample are assumed to emerge from that face. To approximate this condition as closely as possible, the unexposed face of the sample was insulated with 6 mm of ceramic fiber insulation placed on the outside of an aluminum foil wrap. The foil was wrapped on the edges of the sample but, on the unexposed face, there was a gap of 1.5–2 mm which opened to the top of the sample face only. This arrangement approximated the adiabatic back surface condition while allowing gases from the rear face to pass freely to a location where their burning would not feed heat to the sample. In the two-sided burning cases only the sample edge was wrapped with foil to inhibit any tendency for gases to evolve there.

## EXPERIMENTAL RESULTS

Figure 8 shows a typical rate of heat release curve, annotated so as to indicate the various stages of burning of the sample. The sample ignites at 166 s after the start of the irradiation, in this case on one face only. There is essentially immediate involvement of the upper half of the irradiated face but it takes another 17 s for the flame to

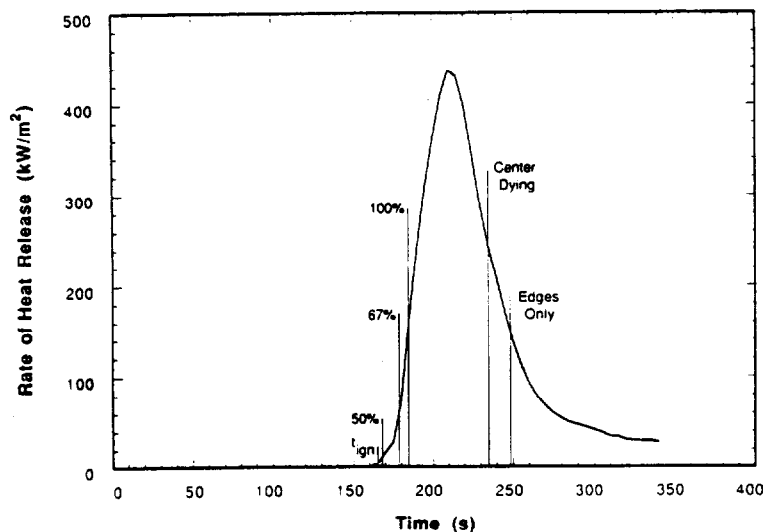


**Figure 8.** Typical experimental rate of heat release curve showing percentage of sample face area which is burning as well as events in the dying out of the burning process. 'Center dying' is the earliest indication that the flames near the center of the sample face are going out.

spread over the full face. Here this full spread is complete well ahead of the peak in the rate of heat release curve. This spread tended to be somewhat slower for the other two materials, but, as noted above, spread was nearly always complete before the peak was reached. On the other side of the heat release peak the video-tapes consistently showed that the central region of the sample extinguished first. The spread between 'center dying' and 'edges only' indicates some ambiguity in the timing of this. The first notation shows the earliest hint that the flames in the center of the sample face were weakening; the second notation indicates the time at which only the periphery of the sample continued to flame.

In addition to these non-one-dimensional effects on the beginning and end of the experimental heat release rate curves there is some distortion (flattening) of the peak due to instrument characteristics. Both flow dispersion in the gas sampling lines of the Cone Calorimeter and the finite response time of the oxygen analyzer (7–8 s for 90% response to a step change) contribute to an overall system response time of about 10–12 s for 90% response to a step change. This is not a significant problem with data such as those in Fig. 8. It is significant (but not large) for the shortest tests (highest flux on two faces of the sample) where the bulk of the heat release peak is only about 30 s long. The underestimate of the true peak height should be less than 10% in these worst cases.

At this point, with the time scales in Fig. 8 in mind, it is pertinent to examine the extent to which the samples behave in a thermally thin manner. Recall that in the ideal case this implies no temperature gradient at all in the depth of the sample. Carslaw and Jaeger<sup>3</sup> present solutions to a relevant heat conduction problem, that of an inert, slab-like sample heated by a constant flux on one face with the other face being adiabatic. As such a sample heats up, it retains a front-to-back temperature difference relative to the increasing average temperature. That fractional difference, divided by the mean temperature, is

given by:

$$\text{Fraction} = 0.5 l_s^2 / (\alpha t) \quad (6)$$

Here  $l_s$  is the sample thickness, as before;  $\alpha$  is the thermal diffusivity of the sample and  $t$  is the time over which the sample has been subjected to the constant front surface heat flux. Note that this fraction decreases with time. Using a value for  $\alpha$  of  $0.19 \text{ mm}^2 \text{ s}^{-1}$  derived from data in reference 4 and the 1.6 mm thickness of the samples used here, one finds

$$\text{Fraction} = 6.7/t \quad (7)$$

At the low end of the flux range used here (approximately  $20 \text{ kW m}^{-2}$ ) the ignition time for one-sided irradiance was of the order of 200 s. At the high end of the flux range (approximately  $40 \text{ kW m}^{-2}$ ) it was as short as 70 s. Assuming ignition occurs at 300–350°C, one finds front-to-back temperature differences at ignition time which are a small fraction of the mean temperature. However, particularly at high fluxes, the inferred differences (approximately 30°C) are not small in terms of their potential effect on the sample degradation/gasification process. The Arrhenius temperature dependence of the chemical reactions serves as a large amplifier of this relatively small temperature difference. Fortunately, the endothermicity of the reactions tends to damp this temperature difference. That is, as soon as the front-to-back temperature difference starts to cause the front to gasify preferentially, the heat absorbed by this reaction slows the local rate of temperature rise and helps bring the front and back of the sample more into temperature equality. The quantitative extent to which this forces a more constant temperature through the sample depth can only be assessed in the context of a thermally thick model. The thermally thin model above shows that the chemical heat sink term is comparable to the thermal capacitance term so the potential for temperature smoothing is there. The holes through the samples, described above, also should help

push toward the idealized behavior of equal mass fluxes from the front and back of the sample. In any event, it is clear that the ideal extreme of thermally thin behavior is approached here but is probably not achieved.

The measured data on each of the materials comprise complete rate of heat release curves at three (or more) flux levels. For present purposes it is sufficient to examine only the behavior of the peak rate of heat release, as was done with the model results in Fig. 6. Figures 9-11 show such results for the three materials described in Table 1. All are plotted on the same scale, though it should be noted that the scales in the plot of the model predictions (Fig. 6) are different. Examination of these figures shows that there is a distinct tendency for the ratio of two-sided to one-sided peak heat release rate to be greater than is predicted by the transient model. The ratio in Figs. 9-11 is greater than two, whereas in Fig. 6 it is less than two. When one recalls that the one-sided peaks should be divided by a factor of two to eliminate the heat release from the gases evolved from the rear surface, the stronger synergistic effect in the two-sided experimental results is even more striking. The ratio of the two-sided to one-sided peaks is then 4-5, as compared to a factor of two expected for thermally thick materials.

The reasons why the experimentally observed synergism is greater than that predicted are not completely clear. It must be borne in mind that the model cannot be expected to be quantitatively accurate since the kinetic parameters it uses have not been measured. In addition, the description of the effects of boundary layer blowing (Eqn (2)) on the flame heat feedback is qualitative at best for these samples with their pattern of holes. The non-ideal effects in the experiments discussed above should have mixed effects. The finite instrument response time will lower the two-sided heat release peaks more than the one-sided peaks but, as indicated above, this effect is probably not appreciable here. The impact of a departure from true thermally thin behavior is harder to judge but its main effect is probably to cause a somewhat greater flow of gasification products out the front face of the sample (versus the back) in the one-sided heating case. Then the one-sided peaks should be divided by a factor somewhat less than two in inferring the ultimate degree of synergism in the above discussion.

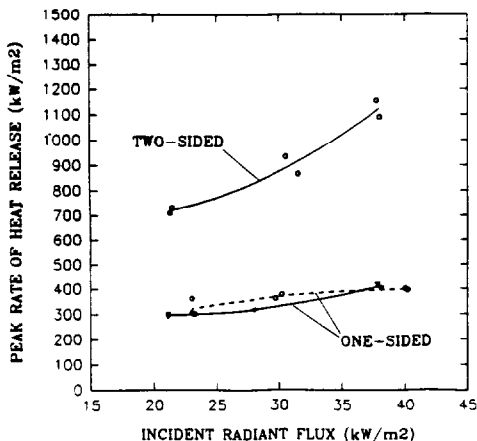


Figure 9. One- and two-sided rate of heat release, G-11 epoxy/glass, 1.6 mm thick.

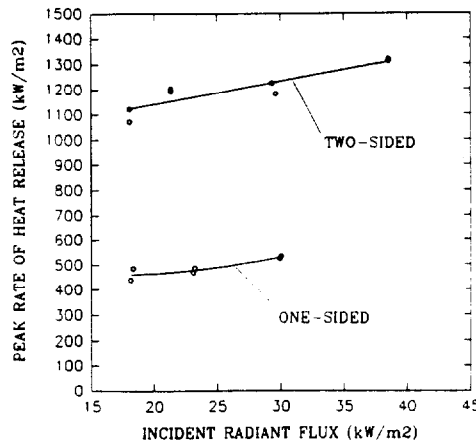


Figure 10. One- and two-sided rate of heat release, Haysite H755 polyester/glass, 1.6 mm thick.

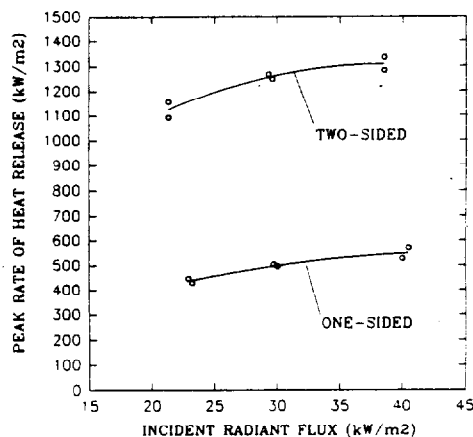


Figure 11. One- and two-sided rate of heat release, Haysite ETS polyester/glass, 1.6 mm thick.

Another secondary factor with a similar effect is variation in flame temperature; recall that it was taken to be constant in the models. The back surface in the one-sided burning case will be less than perfectly adiabatic (though the insulation scheme used should be quite effective); this will somewhat lower the flame temperature. This loss is absent in the two-sided burning case which also has more net energy input via the incoming radiation on the second surface; thus the flame temperature should be relatively higher.

### IMPLICATIONS FOR MATERIAL FLAMMABILITY

The first implication of the synergism is already clear; when a thermally thin material burns it gives off heat at a substantially greater rate than one might expect on the basis of a one-sided burning test. Clearly, however, it must do so for a proportionately shorter time. (The total energy evolved will not be effected but, since the heat

release is a non-constant transient, the reduction in burn time will not necessarily be by the same factor as the change in peak heat release rate.)

The change in peak heat release rate brings with it the possibility that the tendency for flames to spread over the material will be altered. One- and two-sided opposed-flow flame spreads have not been examined in this study but this process is dominated by solid and gas phase heat conduction at the leading edge of the flame. It is not clear that the synergistically enhanced mass flux that would result in the two-sided case would result in an equal (or any) synergism in flame spread rate beyond the factor of two normally expected.

To make an assessment of the possible enhancement of concurrent (e.g. upward) flame spread, the model of Cleary and Quintiere<sup>5</sup> is useful. That model, which is qualitatively applicable to the small-scale, laminar flame conditions of the NASA flammability test, leads to an expression for the critical heat release rate necessary for concurrent flame spread:

$$Q^* = (1/k_f)[(t_{\text{ign}}/t_b) + 1] \quad (8)$$

Here  $Q^*$  is the minimum rate of heat release on the ignited portion of a material for concurrent spread to proceed indefinitely in the direction of gas flow over the material. The quantity  $k_f$  is a proportionality factor between heat release rate and flame length in the direction of spread;  $t_{\text{ign}}$  is the ignition delay time of the material at the flame heat flux;  $t_b$  is the burning time of the material once it is ignited.

Compare the one- and two-sided heating/burning cases in the context of this criterion for concurrent flame spread. To a first approximation the proportionality constant  $k_f$  is the same for both cases. (There are some complications here due to applying a turbulent flame model to the laminar situation that exists in a small scale flammability test; see reference 6.) The ignition delay time at the flame heat flux will differ by a factor of two between the two cases; the two-sided spread case will ignite in half the time since the mass being heated by each flame is halved. The burn time also tends to change by about a factor of two. In the experiments described above the total burn time in the two-sided cases decreased by very

nearly a factor of two in the low-flux cases but the decrease was closer to a factor of three at the high end of the incident flux range. The ratio ( $t_{\text{ign}}/t_b$ ) in Eqn (8) is in the range from about 1.5 (high incident flux) to 5 (low incident flux) for the materials tested here so the high flux changes in  $t_b$  (beyond a simple factor of two) influence  $Q^*$  rather weakly. From the preceding one infers that, for the low incident flux cases,  $Q^*$  is unchanged; for the high incident flux cases it increases less than 50%. Combining this with the strong increases in rate of heat release seen in the two-side cases above, one infers that the two-sided case is always more prone to concurrent flame spread than is the one-sided heating/burning cases since it is more likely to exceed the above criterion for spread.

There is one further subtlety that is pertinent to such testing. When a fixed flaming ignition source, such as the NASA 8060.1C chemical ignition source, is used to test a material in a one-sided versus a two-sided exposure the latter is, in one sense, less severe. Splitting the igniter flame between the two surfaces halves the effective rate of heat release and thus reduces the igniter flame length on the two sides of the sample.<sup>6</sup> The igniter's rate of heat release helps drive the initial flame spread process up the face of a sample and can have a substantial impact on whether the flame spreads beyond a fixed pass/fail length. A completely equitable comparison of one-sided and two-sided ignition and concurrent flame spread hazards would call for two igniters in the two-sided case, one on each side of the sample. Of course, it can be argued that this is a highly improbable occurrence in actual practice.

This study clearly demonstrates that two-sided burning of thermally thin materials is, for the synergistic reasons which emerge from the models above, more hazardous than one-sided burning. Thus it is clearly important to test thin materials in this manner in keeping with the idea of a worst-case assessment of their potential hazard.

#### Acknowledgements

K. Villa provided assistance in some experimental aspects of this program, which was sponsored by NASA Lewis Research Center, Order #C-32003-R.

#### REFERENCES

1. B. Spalding, *Int. J. Heat and Mass Transfer* **1**, 192 (1960).
2. D. Rasbash, D. Drysdale and D. Deepak, *Fire Safety J.* **10**, 1 (1986).
3. H. Carslaw and J. Jaeger, *Conduction of Heat in Solids*, 2nd Edn., p. 112, Clarendon Press, Oxford (1959).
4. ASM International, *Engineered Materials Handbook*, Vol. 1, *Composites*, p. 405, ASM International, Metals Park, Ohio (1987).
5. T. Cleary and J. Quintiere, A framework for utilizing fire property tests. In *Fire Safety Science—Proceedings of the Third International Symposium*, p. 647, Elsevier Applied Science, New York (1991).
6. T. Ohlemiller and K. Villa, Material Flammability Test Assessment for Space Station Freedom. National Institute Of Standards and Technology NISTIR 4591, June (1991) (also NASA CR-187115).